THE JOURNAL OF BIOLOGICAL CHEMISTRY VOL. 287, NO. 35, pp. 29776–29788, August 24, 2012

Complete 6-Deoxy-D-*altro*-heptose Biosynthesis Pathway from *Campylobacter jejuni*

MORE COMPLEX THAN ANTICIPATED[*]

Received for publication, June 11, 2012, and in revised form, July 4, 2012 Published, JBC Papers in Press, July 11, 2012, DOI 10.1074/jbc.M112.390492

Matthew McCallum[‡], **Steven D. Shaw**[‡§], **Gary S. Shaw**[§], **and Carole Creuzenet**[‡1]

From the [‡]*Department of Microbiology and Immunology, Infectious Diseases Research Group, and* [§]*Department of Biochemistry, University of Western Ontario, London, Ontario N6A 5C1, Canada*

Background: Modified heptoses found on the surface of bacterial pathogens may be involved in virulence, but their biosynthesis is poorly understood.
Results: We deciphered the GDP-6-deoxy-D-*altro*-heptose biosynthesis pathway from the human pathogen *Campylobacter jejuni.*
Conclusion: The pathway revealed unexpected activities and complex regulatory features.
Significance: The characterized enzymes can be exploited to synthesize carbohydrate antigens or to develop therapeutic inhibitors.

The *Campylobacter jejuni* capsule is important for colonization and virulence in various infection models. In most strains, the capsule includes a modified heptose whose biological role and biosynthetic pathway are unknown. To decipher the biosynthesis pathway for the 6-deoxy-D-*altro*-heptose of strain 81-176, we previously showed that the 4,6-dehydratase WcbK and the reductase WcaG generated GDP-6-deoxy-D-*manno*-heptose, but the C3 epimerase necessary to form GDP-6-deoxy-D-*altro*-heptose was not identified. Herein, we characterized the putative C3/C5 epimerase Cjj1430 and C3/C5 epimerase/C4 reductase Cjj1427 from the capsular cluster. We demonstrate that GDP-6-deoxy-D-*altro*-heptose biosynthesis is more complex than anticipated and requires the sequential action of WcbK, Cjj1430, and Cjj1427. We show that Cjj1430 serves as C3 epimerase devoid of C5 epimerization activity and that Cjj1427 has no epimerization activity and only serves as a reductase to produce GDP-6-deoxy-D-*altro*-heptose. Cjj1430 and Cjj1427 are the only members of the C3/C5 epimerases and C3/C5 epimerase/C4 reductase families shown to have activity on a heptose substrate and to exhibit only one of their two to three potential activities, respectively. Furthermore, we show that although the reductase WcaG is not part of the main pathway, its presence and its product affect the outcome of the pathway in a complex regulatory loop involving Cjj1427. This work provides the grounds for the elucidation of similar pathways found in other *C. jejuni* strains and other pathogens. It provides new molecular tools for the synthesis of carbohydrate antigens useful for vaccination and for the screening of enzymatic inhibitors that may have antibacterial effects.

Campylobacter jejuni is the leading cause of bacterial gastroenteritis and food-borne disease in the Western world and accounts for 5% of food-related deaths (1, 2). In addition, *C. jejuni* infection is strongly associated with Guillain-Barré syndrome, a rapidly ascending paralysis, as well as inflammatory bowel disease and reactive arthritis (3, 4). Like numerous other bacterial pathogens, *C. jejuni* has developed antibiotic resistance (5–7). This phenomenon may be linked to the fact that *C. jejuni* is commensal in poultry and cattle and that sub-therapeutic antibiotics were used for years to increase productivity (8). This exposure of *C. jejuni* in the commensal host has often offered the bacterium an opportunity to develop antibiotic resistance before transfer to the human host via contamination of the meat during processing or via contamination of water tables from cattle runoffs or insufficiently processed manure (8). This has prompted the need to develop novel and more effective antimicrobials and vaccines (9), which in turn require a better understanding of the mechanisms that sustain the virulence of *C. jejuni*.

Several virulence factors contribute to the pathogenicity of *C. jejuni*, including the flagella that confer motility and are important for colonization (10, 11), the glycosylation of proteins that allows antigen protection/masking (12, 13), and surface glycolipids such as the lipooligosaccharide (14), and the capsule (15) that provide resistance to a wide array of innate immune defenses (16). The capsule is required for diarrheal disease and colonization in animal models of infection, as well as adherence, invasion, and serum resistance in human infections (17). The capsule of *C. jejuni* includes modified heptoses that can be C6-dehydrated or *O*-methylated on C6 hydroxyl and that can be present in a variety of ring configurations (18–22). For example, 6-*O*-methyl-L-*gluco*-heptose and 6-deoxy-D-*altro*-heptose have been identified in *C. jejuni* NCTC 11168 and 81-176, respectively (19, 22). Although it has been demonstrated that *C. jejuni* mutants deficient in capsule production have an altered immunoreactivity (23) and have a drastically diminished capacity to colonize 1-day-old chicks (24), the precise role of the heptose modification is unknown. The heptose

[*] This work was supported by Natural Sciences and Engineering Research Council of Canada Operating Grant RGPIN 240762-2010 (to C. C.) and Canadian Institutes of Health Research Grant MOP 93520 and the Canada Research Chairs Program (to G. S. S.).
[1] To whom correspondence should be addressed: Dept. of Microbiology and Immunology, Infectious Diseases Research Group, University of Western Ontario, DSB 3031, London, Ontario N6A 5C1, Canada. Tel.: 519-661-3204; Fax: 519-661-3499; E-mail: ccreuzen@uwo.ca.

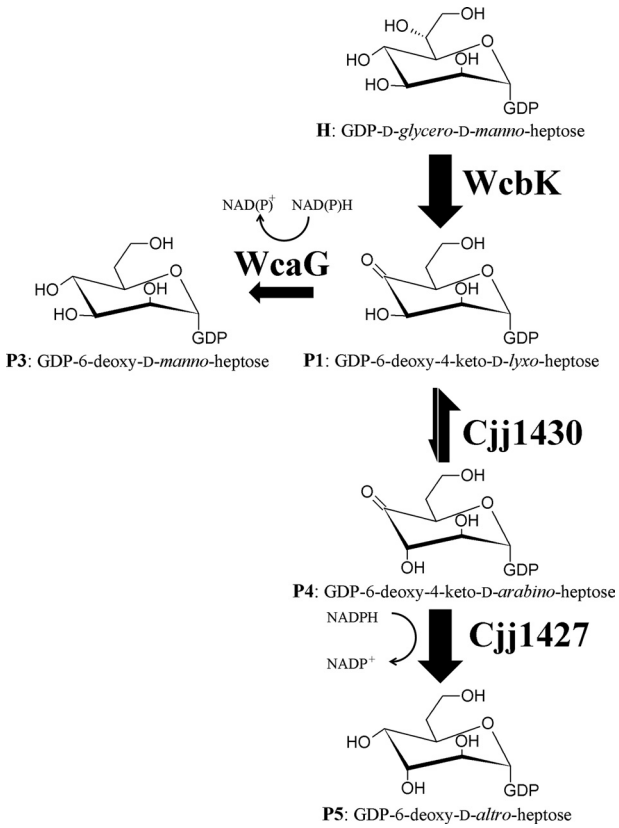

FIGURE 1. **GDP-6-deoxy-D-*altro*-heptose synthesis pathway in *C. jejuni* 81-176.** The pathway results from the combination of the CE, MS, and NMR spectroscopy analyses described in these studies. The *thickness* of the *arrows* represents the catalytic efficiency of the specified reaction.

modification may contribute to capsular function, as was previously observed in *Yersinia pseudotuberculosis* (25, 26). Answering this question requires elucidation of the heptose modification pathway, which our laboratory has been addressing via biochemical and genetic approaches. The biochemical characterization of the enzymes will determine unambiguously the role of each capsular gene in the modification pathway and ultimately will allow using the enzymes as novel targets for the development of therapeutic inhibitors. These enzymes could also be used to produce biosynthetic carbohydrates that could serve as epitopes for vaccination. Although the chemical synthesis of a modified heptose was recently described, it is quite difficult and cumbersome (27), and enzymatic synthesis represents an appealing alternative, being more efficient and malleable.

We reported recently the biochemical characterization of the C6 dehydratase WcbK and C4 reductase WcaG that had been identified in the capsular gene cluster of *C. jejuni* strain 81-176 by homology with the *Y. pseudotuberculosis* heptose-modifying enzymes DmhA and DmhB (28, 29). Our biochemical characterization of WcbK and WcaG showed that WcbK can dehydrate GDP-D-*glycero*-D-*manno*-heptose (herein referred to as GDP-*manno*-heptose) to produce compound P1, the anticipated precursor for GDP-6-deoxy-D-*altro*-heptose (18), and that its reaction product can be reduced by WcaG to yield product P3 (Fig. 1). As monitored by NMR spectroscopy, these activities did not give rise to the expected C3 epimerization step necessary to generate the D-*altro* epimer that is found in the capsule. This indicated that at least one more enzyme is involved in the required C3 epimerization step. Moreover, the k_{cat} of WcbK on GDP-*manno*-heptose was low in comparison with the k_{cat} of DmhA on the same substrate (29). This suggested that WcbK may have a higher k_{cat} on the C3-epimerized (*altro*) heptose, implying an alternate enzymatic order for the heptose modification pathway that may not be led by WcbK. However, structural modeling data argued against this hypothesis. Therefore, it was necessary to identify the putative C3 epimerase of the complete biosynthesis pathway and to determine unambiguously the sequence of the reactions.

To date, no GDP-*manno*-heptose C3 epimerase has been characterized. Cjj1430 and Cjj1427 are the only enzymes with putative C3 epimerase activity present in the capsular gene cluster of *C. jejuni* strain 81-176 (18). Specifically, Cjj1430 is similar to the dTDP-6-deoxy-D-*xylo*-4-hexulose C3/C5 epimerases RmlC from *Escherichia coli* (26% identical, 57% similar) and RfbC from *Salmonella enterica* (30% identical, 59% similar), which are involved in dTDP-L-rhamnose synthesis (30–32). Cjj1427 is similar to the GDP-fucose synthases from *E. coli* (31% identical, 70% similar) and *Helicobacter pylori* (44% identical, 59% similar), which are GDP-4-keto-6-deoxy-α-D-mannose C3/C5 epimerases/C4 reductases (GMER)[2] involved in the formation of GDP-L-fucose (33, 34). Although both Cjj1430 and Cjj1427 are predicted to have C3/C5 epimerase activities, Cjj1430 is a rather small protein of 181 amino acids, and Cjj1427 is a large protein of 352 amino acids, and they exhibit little similarity with one another (13% identity, 30% similarity). Therefore, their functions are not anticipated to be redundant.

We hypothesized that both Cjj1430 and Cjj1427 would be involved with the generation of the capsule-linked D-*altro*-heptose in *C. jejuni* strain 81-176. In this work, we cloned, overexpressed, and purified the yet uncharacterized Cjj1430 and Cjj1427 enzymes from *C. jejuni* strain 81-176, identified the order of the enzyme activities in the complete GDP-6-deoxy-D-*altro*-heptose modification pathway with respect to WcbK and WcaG, and determined the reactions catalyzed by each enzyme along the pathway using a combination of capillary electrophoresis, mass spectrometry, and NMR spectroscopy analyses.

MATERIALS AND METHODS

Cloning of cjj1427 and cjj1430 into the pET Vector—The *cjj1427* and *cjj1430* genes from *C. jejuni* strain 81-176 were PCR-amplified from genomic DNA using primers CJPGFclP1 (AGGTACCATGGGCATGCAAAAAGATTCTAAAAATT) and CJPGFclP2 (GCTGGATCCCTATTGTCTTATATTTTGCT) for *cjj1427* and primers CJPG1430P1 (AGGTACCATGGGCATGGCAAAGAATTTAATATAC) and CJPG1430P2 (GCTGGATCCTTATCCTTTATTTTTATTGCT) for *cjj1430*. The PCR was accomplished using PfuTurbo DNA polymerase (Stratagene) according to the manufacturer's instructions, with annealing at 50 °C for *cjj1430* and 45 °C for *cjj1427*. The PCR products were digested with NcoI and BamHI and were cloned into the pET23

[2] The abbreviations used are: GMER, GDP-4-keto-6-deoxy-α-D-mannose C3/C5 epimerases/C4 reductases; CE, capillary electrophoresis.

derivative (35) with an N-terminal hexahistidine tag. The recombinant plasmids were transformed into *E. coli* DH5α with ampicillin selection (100 μg/ml). The resulting plasmids pET-*cjj1427* and pET-*cjj1430* were purified using the GFX kit (GE Healthcare) and were verified by DNA sequencing (Robarts Institute Sequencing Facility, London, Canada). The cloning of WcbK and WcaG in the pET vector was reported previously (28).

Protein Expression and Purification—Expression was performed in *E. coli* ER2566 for Cjj1427 and *E. coli* BL21(DE3)pLysS for WcbK, WcaG, and Cjj1430, using LB containing 100 μg/ml ampicillin and 34 μg/ml chloramphenicol as appropriate. Protein expression was induced by the addition of 0.1 mM isopropyl β-D-1-thiogalactopyranoside, and expression was carried out at 37 °C, except for Cjj1430 (25 °C). At the end of the induction period, the cells were harvested by centrifugation (8000 × *g*) and stored at −20 °C until needed.

Purification of Histidine-tagged Proteins by Nickel Chelation—The induced cell pellets were resuspended in binding buffer (0.1 M NaCl, 20 mM imidazole, 20 mM Tris-HCl adjusted at pH 8 for WcbK and pH 7 for all other enzymes). After mechanical disruption, the histidine-tagged proteins were purified by nickel chelation using a 1.6 ml of Poros MC 20 column (4.6 × 100 mm; Applied Biosystems) as described previously (28, 29). The protein fractions of interest were analyzed by SDS-PAGE and Coomassie staining and were stored in a final concentration of 25% glycerol at −20 °C.

Capillary Electrophoresis (CE) of Sugar Nucleotides—CE was performed on a Beckman Gold instrument using a 57-cm bare silica capillary and separation with 200 mM borax buffer, pH 9, under 26 kV as described previously (28, 29). Substrate conversion was estimated by integration of the surface areas under the substrate and product peaks detected at 254 nm using the 32 Karat software.

Preparation of GDP-D-Glycero-D-manno-heptose—The enzymatic preparation of GDP-D-*glycero*-D-*manno*-heptose from sedoheptulose 7-phosphate was performed as reported previously (28, 29). The reaction product that served as a substrate in this work was purified by anion exchange chromatography as described below.

Purification of Sugar Nucleotides—Sugar nucleotides were purified by anion exchange chromatography using a High Q EconoPac 1-ml column (Bio-Rad) and a linear gradient of triethylammonium bicarbonate, pH 8.5 (50 mM to 1 M), at 1 ml/min with UV detection (28, 29). The fractions containing the product of interest were pooled and lyophilized twice in water. Quantification was performed using a Nanodrop spectrophotometer and using $\epsilon_{GTP} = 12000\ mol^{-1}\ liter\ cm^{-1}$.

Enzyme Assays—All reactions contained ~0.10 mM substrate, 0.12 mM NADPH/$NADP^+$ mix (70:30%) in 200 mM Tris-HCl, pH 8.0, and were incubated at 37 °C. The amounts of enzymes added and incubation times are specified in the legends to the figures. The reaction products were analyzed by CE as described above. Large scale reactions were prepared by direct proportional increase of all components for anion exchange purification followed by MS or NMR spectroscopy analyses.

MS Analysis of Reaction Products—Enzymatic reactions were linearly scaled up to contain ~3 nmol of the product and were performed in volatile ammonium bicarbonate buffer instead of Tris-HCl. They were lyophilized in H_2O twice before MS analysis. Alternatively, purified reaction products were analyzed by MS.

For deuterium incorporation experiments, in a first set of analyses, the WcbK reaction was performed in buffer prepared in D_2O, and once full conversion to P1 was observed (as per CE analysis), Cjj1430 was added so that its reaction also occurred in D_2O. The enzymes were removed by ultrafiltration (membrane cutoff of 3 kDa). In a second set of analyses, the WcbK reaction was performed in H_2O; the enzyme was filtered out by ultrafiltration, and the product was lyophilized. The product was rehydrated in D_2O, and Cjj1430 that had been washed in deuterated buffer by ultrafiltration was added to the rehydrated P1 product. After the Cjj1430 reaction had occurred in D_2O, the enzyme was removed by ultrafiltration. All final samples were lyophilized to near dryness and rehydrated in H_2O three times before MS analysis. All reaction products were analyzed by LC-MS/MS at the Rix Protein Identification Facility of the University of Western Ontario in the negative ion mode as reported before (28, 29).

MALDI MS Analyses of Purified Enzymes—MALDI MS analyses were performed at the MALDI mass spectrometry facility of the University of Western Ontario using a 4700 Proteomics Analyzer (Applied Biosystems, Foster City, CA) in the linear positive ion mode as described before (29).

NMR Spectroscopy—Large scale reactions were performed using 0.75 μmol of GDP-*manno*-heptose, 0.87 μmol of NADH, 0.20 μg of WcbK, 0.26 μg of Cjj1430, 0.24 μg of Cjj1427, and 0.30 μg of WcaG (as appropriate) in 6.25 ml of 0.2 M triethylammonium bicarbonate, pH 8.5. The reactions were incubated for 1 h at 37 °C. The reactions were filtered through a 3-kDa cutoff ultrafiltration centrifugal device (Pall Filtron) to remove the enzymes, and the reaction products were purified by anion exchange chromatography as described above. The purity of the fractions was monitored by CE. The purified products (P5 and P6) were lyophilized repeatedly after resuspension in Milli Q water (twice) and in D_2O (four times).

All ^1H NMR data were collected with a Varian Inova 600 MHz NMR spectrometer at 25 °C. ^1H NMR spectra were collected using a 2-s presaturation pulse for products P5 and P6, or WET sequence (36) for P3, centered on the residual HDO resonance. ^1H and ^{13}C assignments for the reaction products were determined from a two-dimensional ^1H TOCSY experiment (37), using a 6-Hz spin lock for 256 complex increments and natural abundance ^1H-^{13}C HSQC experiment (38, 39). In addition, selective one-dimensional ^1H TOCSY and NOESY experiments were used to confirm assignments and arrangement of the pyranose ring. All spectra were processed using unshifted Gaussian weighting in VnmrJ 2.1B and ^1H and ^{13}C chemical shifts referenced to 2,2-dimethyl-2-silapentane-5-sulfonate sodium salt at 0.00 ppm.

RESULTS

Expression and Purification of C. jejuni 81-176 WcbK, WcaG, Cjj1430, and Cjj1427—The overexpression, purification, and characterization of WcaG and WcbK were performed as

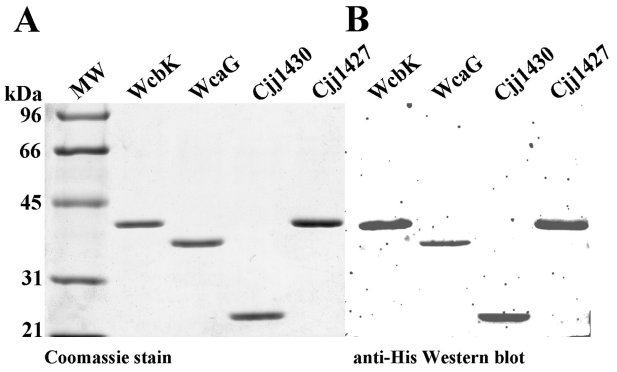

FIGURE 2. **SDS-PAGE analysis of purified WcbK, Cjj1430, Cjj1427, and WcaG.** The proteins were purified by nickel affinity chromatography. Detection was performed with Coomassie staining (*A*) and anti-histidine tag Western blotting (*B*). *MW*, molecular weight. The WcbK, WcaG, and Cjj1427 proteins migrated at their expected molecular masses of 40.5, 36.5, and 41.7 kDa, respectively. Cjj1430 migrated at a higher molecular mass than expected (22.1 kDa).

reported previously (28). Similar results were obtained in this work (Fig. 2). Like WcaG and WcbK, Cjj1430 and Cjj1427 were also overexpressed in *E. coli* with an N-terminal histidine tag using the pET system. High yields of soluble proteins were obtained. The proteins were purified to near-homogeneity in a single step of nickel affinity chromatography and reacted with the anti-His antibody (Fig. 2). Although Cjj1427 migrated to the expected size of 41.7 kDa on SDS-polyacrylamide gels, Cjj1430 migrated close to 25 kDa, although it was expected at 22.1 kDa (Fig. 2). MALDI MS analysis indicated that both Cjj1427 and Cjj1430 proteins had the expected molecular weight, despite the anomalous migration of Cjj1430 on SDS-polyacrylamide gels.

GDP-6-Deoxy-D-altro-heptose Synthesis Pathway Is Initiated by WcbK—We previously demonstrated that WcbK can dehydrate GDP-*manno*-heptose to generate GDP-6-deoxy-4-keto-heptose, referred to as P1 (Fig. 1) (28). However, the k_{cat} of this reaction is slightly lower than that of DmhA, a similar GDP-*manno*-heptose C6 dehydratase in *Y. pseudotuberculosis* (28, 29). This raised the possibility that GDP-*manno*-heptose was not the preferred substrate of WcbK and that the epimerization step necessary to produce the *altro* ring configuration may actually occur before C6 dehydration by WcbK *in vivo*. Hence, the potential epimerization activities of Cjj1427 and Cjj1430 on GDP-*manno*-heptose were examined by CE, using UV absorbance to monitor the GDP portion of the GDP-linked heptose. No novel product was observed, indicating that Cjj1427 and Cjj1430 did not catalyze the GDP-*manno*-heptose substrate (data not shown). Likewise, we demonstrated earlier that WcaG has no activity on GDP-*manno*-heptose (28). Therefore, these data demonstrate that the GDP-6-deoxy-D-*altro*-heptose synthesis pathway is initiated by WcbK as highlighted in Fig. 1.

Neither Cjj1430 Nor Cjj1427 Use the WcaG/WcbK Reaction Product P3 as a Substrate—As we have shown previously, WcaG can use NAD(P)H to reduce the 4-keto group of the WcbK reaction product P1 to generate P3 (Figs. 1 and 3*A*, *trace d*) (28). However, NMR spectroscopy has demonstrated that C3 of this WcaG product remains nonepimerized so that the sugar is GDP-6-deoxy-D-*manno*-heptose. It is not in the D-*altro* configuration that is present in the capsule of strain 81-176 (28).

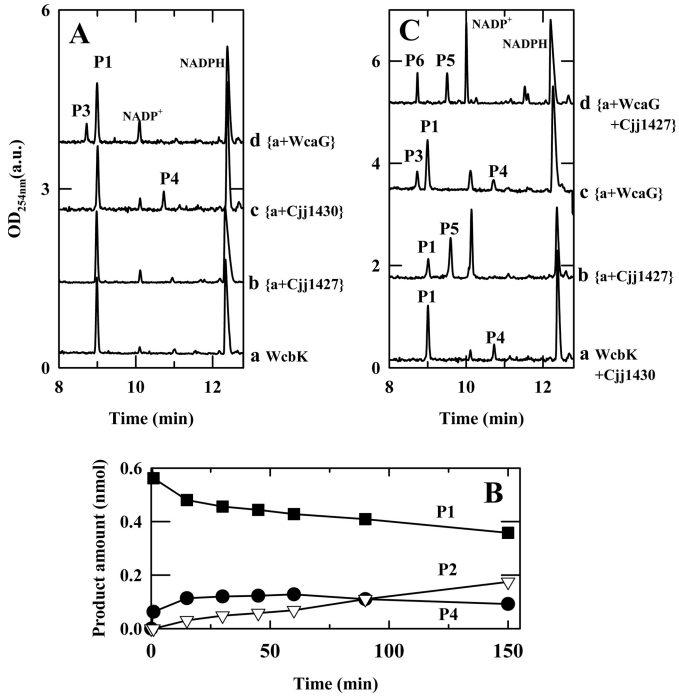

FIGURE 3. **WcaG and Cjj1430 both use the WcbK product P1 as a substrate and Cjj1427 uses the Cjj1430 product P4 as a substrate.** *A*, identification of enzymes that use P1 as a substrate by CE. Each reaction contained ~0.13 mM P1 (derived from WcbK, which was still present at 4 μM) and either 3 μM Cjj1427 (*trace b*), 7 μM Cjj1430 (*trace c*), or 7 μM WcaG (*trace d*), or no additional enzyme (*trace a*). They were incubated for 30 min. New products P3 and P4 were formed in the presence of WcaG and Cjj1430, respectively, but not in the presence of Cjj1427. *B*, time course analysis of Cjj1430 reactions suggesting that Cjj1430 catalyzes an equilibrium reaction. A 36-μl reaction containing 0.14 mM GDP-*manno*-heptose and 0.12 nmol of WcbK was incubated for 15 min for full conversion to P1. Cjj1430 (0.03 nmol) was added, and the reaction progress was monitored by CE analysis. Quantitation of product formation was obtained by peak area integration. The data are representative of two independent experiments. P1, *closed* squares; P2, *open triangles*; P4, *closed circles*. *C*, capillary electrophoregrams showing that Cjj1427, and not WcaG, uses P4 as a substrate and that all four enzymes lead to the formation of new product P6. Each reaction initially contained ~0.10 mM P1 and 0.02 mM P4 (derived from WcbK and Cjj1430, which were still present and active in the reaction at 3 and 6 μM). The reactions were incubated for 30 min as such (*trace a*, no additional enzymes) or were supplemented with either 6 μM Cjj1427 (*trace b*), WcaG (*trace c*) or both Cjj1427 and WcaG (*trace d*) before incubation.

This suggested that P3 may subsequently be epimerized on C3 by additional enzymes such as Cjj1430 or Cjj1427. Therefore, the activities of Cjj1427 and Cjj1430 on P3 were assessed by CE. No new product peak was detected with the addition of Cjj1430 or Cjj1427, even in the presence of cofactor, indicating that P3 is not catalyzed by Cjj1430 or Cjj1427 (data not shown).

Cjj1430 Uses the WcbK Reaction Product P1 as a Substrate to Generate P4—Because the data above indicated that neither Cjj1430 nor Cjj1427 used P3 as a substrate, and P3 was not in the proper configuration to lead to the *altro*-heptose derivative present in the capsule, it was likely that Cjj1430 and/or Cjj1427 could convert P1 into an *altro* form before its final reduction. Hence, the ability of Cjj1427 and Cjj1430 to catalyze P1 was assessed by CE analysis. When P1 was incubated with Cjj1427, no catalysis was observed, indicating that Cjj1427 did not use P1 as a substrate (Fig. 3*A*, *trace b*). In contrast, when P1 was incubated with Cjj1430, the formation of a novel reaction product P4 was observed, concurrently with a stoichiometric decrease in P1 (Fig. 3*A*, *trace c*). P4 was not present in control

reactions where Cjj1430 was omitted or when Cjj1430 was present and P1 was absent. These data indicate that Cjj1430 used the reaction product of WcbK (P1) as a substrate (Fig. 1).

Regardless of the concentration of Cjj1430 added, and of the time allotted for catalysis, the maximum production of P4 represented 20–25% of the total GDP-D-*glycero*-D-*manno*-heptose used for the reaction, even when large amounts of P1 were still present (Fig. 3*B*). The reaction yield and the reaction kinetics were not improved when NAD(P)H and NAD(P)$^+$ were added to the reaction. Over time, P1 is known to breakdown noncatalytically to release its GDP moiety (annotated as P2) (28). Interestingly, as P1 broke down into P2, there was a corresponding decrease of P4 levels (Fig. 3*B*). This suggested that the Cjj1430 reaction product P4 is also unstable and breaks down over time to contribute to the rise in P2 levels observed after long incubation times and/or that Cjj1430 catalyzed an equilibrium reaction between P1 and P4.

P4 was detected at *m*/*z* 616 by MS analysis. This *m*/*z* ratio and its MS/MS spectrum were identical to those observed previously for the 6-deoxy-4-keto intermediate P1 generated by WcbK (28) and which is used by Cjj1430 to form P4 (Fig. 4*A*). This is consistent with the following facts: (i) Cjj1430 was predicted to perform an epimerization reaction; (ii) Cjj1430 acted on a pre-formed 4-keto intermediate, and therefore no hydride extraction was needed to carry out the predicted epimerization reaction; and (iii) no cofactor was required for the activity of Cjj1430, and therefore, no reduction of the substrate was anticipated.

Cjj1427 Uses the Cjj1430 Reaction Product P4 as a Substrate to Generate P5—When the P1/P4 mixture from WcbK/Cjj1430 reactions was incubated with Cjj1427 in the presence of NAD(P)H, the formation of a novel reaction product, P5, was observed concurrently with the stoichiometric decrease in the P1 and P4 peaks (Fig. 3*C*, *trace b*). The P5 peak was not present in reactions when Cjj1427 was omitted or when Cjj1430 was omitted. The reaction was dependent on the presence of reduced cofactors NAD(P)H and led to the production of NAD(P)$^+$. Far greater substrate conversion was obtained in the presence of NADPH rather than NADH indicating that the preferred cofactor of Cjj1427 is NADPH. Because P1 is not a substrate for Cjj1427, these data altogether indicate that Cjj1427 uses the Cjj1430 product P4 as a substrate in an oxidoreduction reaction that oxidizes the NAD(P)H cofactor provided (Fig. 1).

MS analysis identified the Cjj1427 reaction product P5 at 618 *m*/*z*, which by MS/MS yielded a fractionation pattern consistent with the predicted C4 reductase activity of Cjj1427 (Fig. 4*B*). It could not be excluded at this stage that P5 also underwent C3/C5 epimerizations compared with the original substrate P4.

Cjj1430 Catalyzes an Equilibrium Reaction between P1 and P4—Interestingly, when Cjj1427 was added to a P1/P4 mixture that contained active Cjj1430 in the presence of NADPH, not only did the Cjj1430 product P4 disappear but also the P1 peak decreased considerably (Fig. 3*C*, *trace b*), although P1 is not a substrate for Cjj1427 (Fig. 3*A*, *trace b*). These data confirm that P4 is used by Cjj1427 as demonstrated above, and they also indicate that Cjj1430 was catalyzing an equilibrium reaction between P1 and P4, as suspected from the data presented in Fig.

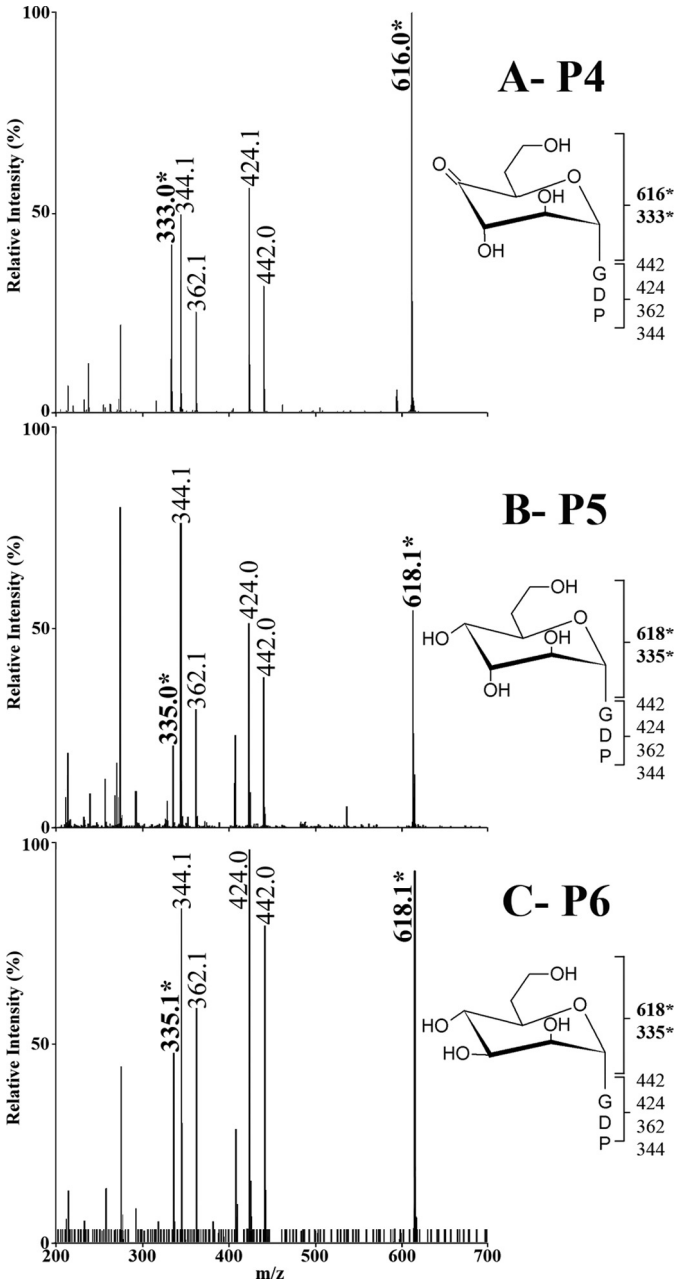

FIGURE 4. **Mass spectrometry analysis of the reaction products P4, P5, and P6.** The MS/MS spectra of the reaction products were obtained from full reactions comprising WcbK and GDP-D-*glycero*-D-*manno*-heptose plus Cjj1430 (*A*, product P4), Cjj1430 and Cjj1427 (*B*, product P5), or Cjj1430, Cjj1427 and WcaG (*C*, product P6). For all panels, the structure of the expected sugar is depicted along with the fractionation pattern that yields peaks present on the MS/MS spectra. Peaks highlighted in bold and with an *asterisk* indicate peaks comprising the heptose ring.

3*B*. The consumption of P4 by Cjj1427 appears to pull the Cjj1430 P1/P4 equilibrium toward production of more P4, therefore consuming more P1 than in the absence of Cjj1427 (see Fig. 1 for the full pathway). Considering that these assays were performed with more than twice as many moles of Cjj1430 than Cjj1427, these data also suggest that in this pathway the reaction catalyzed by Cjj1430 is rate-limiting.

WcaG Cannot Use the Cjj1430 Reaction Product P4 as a Substrate—In parallel reactions performed on the Cjj1430 reaction product P4 with WcaG instead of Cjj1427, P4 was still

TABLE 1
^{1}H and 13C NMR data for the P3, P5, and P6 products of the GDP-6-deoxy-D-*altro*-heptose synthesis pathway
Data for GDP-*glycero*-D-*manno*-heptose (H) are provided as a reference (29).

Compound	^{1}H and ^{13}C chemical shifts[a] (ppm) and coupling constants (Hz)						
	1	2	3	4	5	6	7
P3							
^{1}H	5.45	4.03	3.89	3.50	3.87	2.07, 1.67	3.75, 3.67
$^3J_{HH}$ ($^3J_{HP}$)	1.7 (7.4)	3.0	8.7	9.7			
^{13}C	99.1	73.0	72.9	73.1	72.9	36.2	60.8
P6							
^{1}H	5.44	4.02	3.87	3.50	3.88	2.08, 1.66	3.75, 3.69
$^3J_{HH}$ ($^3J_{HP}$)	1.7 (7.4)	3.5	9.5	9.5			
^{13}C	99.1	73.2	73.6	73.1	73.2	36.3	60.8
P5[b]							
^{1}H	5.32	3.93	3.94	3.70	4.18	1.99, 1.74	3.77, 3.71
$^3J_{HH}$ ($^3J_{HP}$)	2.3 (7.7)	3.7	3.1	8.2			
^{13}C	98.5	72.6	73.0	71.0	70.5	35.5	60.7
H							
^{1}H	5.50	4.02	3.90	3.76	3.88	3.99	3.74
$^3J_{HH}$ ($^3J_{HP}$)	1.6 (7.8)	2.8	10.3	10.4	3.5		
^{13}C	99.1	72.9	76.6	64.7	72.8	74.9	62.2

[a] Chemical shifts were referenced to internal 2,2-dimethyl-2-silapentane-5-sulfonate sodium salt standard, ^{1}H = 0.00 ppm. Only chemical shifts from the sugar portions of the compounds are reported.
[b] Chemical shifts for GDP portion of P5 in ppm are as follows: H1′ (5.93, 89.6); H2′ (4.79, 76.3); H3′ (4.52, 73.2); H4′ (4.34, 86.6); H5′ (4.20, 68.1).

present, although a new product appeared upstream of P1 (Fig. 3*C*, *trace c*). This new product co-migrated precisely with P3, indicating that WcaG catalyzed conversion of P1 into P3 as observed previously and did not use P4. Importantly, under these parallel reaction conditions, WcaG catalyzed approximately two times less P1 than the Cjj1430/Cjj1427 combination did (Fig. 3*C*). This suggests that Cjj1430 and Cjj1427, but not WcaG, preferentially bind and catalyze P1 in the physiological 6-deoxy-D-*altro*-heptose synthesis pathway, whereas the WcaG-mediated conversion of P1 into P3 represents a side branch (Fig. 1). Finally, it was also noted that during the generation of P3 from P1 by WcaG, significant degradation of P1 occurred if reactions were incubated over 1 h at 37 °C. This is in contrast to Cjj1430 and Cjj1427 reactions with P1 in which minimal degradation of P1 was observed during the generation of P5 (data not shown). This further suggested that the generation of P3 is slow and not physiologically preferential in comparison with the rapid generation of P4 and P5.

WcaG Generates P6 in a Cjj1427-dependent Manner but Does Not Use the Cjj1427 Product as a Substrate—As mentioned above, reactions comprising GDP-*manno*-heptose, WcbK, Cjj1430, and Cjj1427 lead to the formation of product P5 in the presence of reduced cofactor NAD(P)H. Concurrent addition of WcaG to such reactions led to the formation of a novel reaction product P6, accompanied by reduced formation of P5 (Fig. 3*C*, *trace d*). Full conversion of the GDP-*manno*-heptose substrate into P6 could be obtained under these conditions (data not shown). Because we showed above that WcaG cannot use the Cjj1430 reaction product P4 as a substrate, and only generates P3 out of the WcbK reaction product P1, these data could at first glance indicate that WcaG uses the P5 Cjj1427 reaction product as a substrate to generate P6. This interpretation is particularly appealing because in the absence of Cjj1427, the WcaG-mediated P1 to P3 conversion is very slow so that most P1 compound decomposes into P2. In contrast, in Cjj1427-containing reactions (also containing all other enzymes), efficient WcaG-mediated formation of the final product P6 was observed with hardly any formation of P2.

However, when the stable P5 Cjj1427 reaction product was purified by anion exchange chromatography and incubated with WcaG, no catalysis was observed, even in the presence of reduced cofactors and of large amounts of WcaG, and upon long incubation times (data not shown). This establishes that the P5 Cjj1427 reaction product is not a substrate for WcaG. This is consistent with the fact that P5 is already a reduced compound and WcaG is a reductase that could not possibly use P5 as a substrate.

Identity of the WcaG Reaction Product P6—As P6 was generated via the combined activity of the four candidate biosynthetic enzymes encoded by the genomic capsular cluster, it was anticipated that P6 would be the final product of the pathway, *i.e.* GDP-6-deoxy-D-*altro*-heptose. But the fact that P6 did not arise directly from WcaG-mediated catalysis of the Cjj1427 product P5 cast doubt on this assignment. Moreover, P6 co-migrated with P3 by CE analysis (Fig. 3*C*, *traces c* and *d*), although CE has enough resolution power that it can discriminate between epimers (40, 41). This suggested that P3 and P6 may be identical compounds and called for MS and NMR spectroscopy analyses. The P6 product was detected at *m*/*z* 618 by mass spectrometry (Fig. 4*C*), and its MS/MS pattern was identical to that of the reduced GDP-6-deoxy-*manno*-heptose isomer P3 obtained upon reduction of P1 by WcaG (28), indicating that P6 is also a reduced compound as expected. Like P3, P6 had an MS/MS pattern consistent with that expected for GDP-6-deoxy-D-*altro*-heptose. Further analysis by NMR spectroscopy clearly demonstrated that P3 and P6 were identical compounds (Table 1 and Fig. 5). Specifically, the chemical shifts for all ^{1}H shifts for P6 were within 0.02 ppm compared with P3, including a characteristic downfield shift for H2 (4.02 ppm) and upfield shift for H4 (3.50 ppm). In addition, large coupling constants were noted for H3, H4 ($^3J_{3,4}$ = 9.5 Hz) and H4, H5 ($^3J_{4,5}$ = 9.5 Hz) indicating these three protons existed in *trans* arrangements around the pyranose ring (42). Comparison of the ^{1}H spectra for P3 and P6 (Fig. 5) showed they were nearly identical.

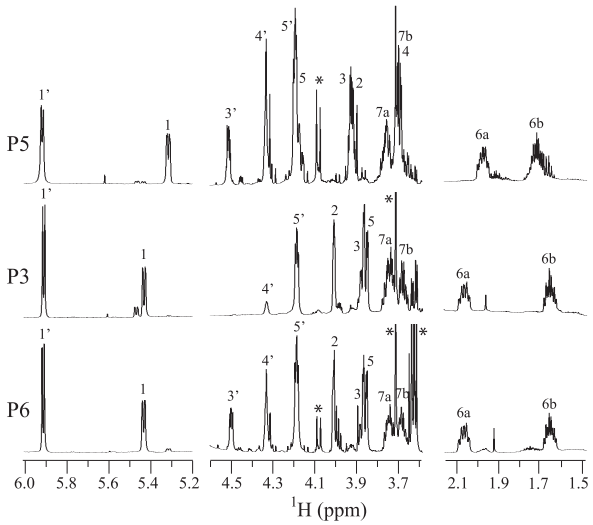

FIGURE 5. **Identification of P5 and P6 using ^{1}H NMR spectroscopy.** Selected regions of the 600 MHz ^{1}H NMR spectra for P5 (*top*) and P6 (*lower*) were prepared as described under "Materials and Methods." The ^{1}H spectrum of P3 (GDP-6-deoxy-D-*manno*-heptose, *middle panel*) that was obtained via the activity of DmhA/DmhB is provided for comparison purposes because we showed previously that WcbK/WcaG or the *Y. pseudotuberculosis* homologues DmhA/DmhB can be used interchangeably to produce P3 (28). Each spectrum shows the ^{1}H assignments for the pyranose (1–7) and ribose (1′-5′) portions of the molecules determined from selective and two-dimensional ^{1}H TOCSY experiments. Differences in the intensities of H3′ and H4′ occur due to the different water suppression methods used. *Peaks* labeled * arise from small amounts of buffer impurities.

NMR Spectroscopy Analysis of the P5 Reaction Product Indicates That WcaG Is Not Part of the Mainstream GDP-6-Deoxy-D-altro-heptose Synthesis Pathway—Because the P6 product obtained upon activity of all four enzymes was not the expected final *altro*-heptose derivative, and involvement of two reductases (Cjj1427 and WcaG) in the pathway was not consistent with the anticipated reaction scheme, we investigated whether the P5 WcbK/Cjj1430/Cjj1427 product was the *altro*-heptose derivative by NMR spectroscopy.

The ^{1}H and ^{13}C chemical shift assignments for P5 (Table 1) were determined using two-dimensional TOCSY spectra, selective one-dimensional ^{1}H TOCSY spectra, and ^{1}H,^{13}C HSQC data. An unusual feature of the data were the downfield-shifted ^{1}H resonance for H5 (4.18 ppm) compared with this proton in either P3 or P6. Similar chemical shifts have been observed for deoxy-*altro*, *ido*, *galacto*, and *talo*-heptoses (42). Further comparisons to chemical shifts for H2 (C2), H3 (C3), and H4 (C4) were most similar to the *altro* form of the sugar. Analysis of ^{1}H,^{1}H coupling constants revealed small couplings between H1,H2 ($^3J_{1,2}$ = 2.3 Hz), H2,H3 ($^3J_{2,3}$ = 3.7 Hz), and H3,H4 ($^3J_{3,4}$ = 3.1 Hz) that was evident from the collapsed nature of these resonances in the ^{1}H spectrum (Fig. 5). This shows that a *trans* arrangement does not exist between any of these proton pairs around the sugar ring. To confirm the 6-deoxy-D-*altro*-heptose configuration, selective one-dimensional ^{1}H NOE experiments were completed. These experiments showed interactions between H1 with H2, H4 with H3 and H6, and H5 with H6 that are in agreement with the *altro* configuration and inconsistent with other arrangements. The absence of NOEs between H3 and H5 also indicated that these protons were not on the same side of the ring as found in the *talo*- and *galacto*-heptoses.

Altogether, these data clearly establish that the sequential activities of WcbK, Cjj1430, and Cjj1427 are sufficient to produce GDP-6-deoxy-D-*altro*-heptose from GDP-6-deoxy-*manno*-heptose. These data also confirm that the extra enzyme WcaG that is encoded in the close proximity of the *wcbK*, *cjj1430c,* and *cjj1427* genes in the capsular cluster is not involved in the mainstream pathway.

Two Putative C3/C5 Epimerases Involved in a Single C3 Epimerization Step? Implication for Functional Assignments—The data presented above involve both Cjj1430 and Cjj1427 in GDP-6-deoxy-D-*altro*-heptose synthesis. Cjj1430 is similar to well characterized dTDP-6-deoxy-D-xylo-4-hexulose C3/C5 epimerases involved in dTDP-L-rhamnose synthesis (30–32), and Cjj1427 is similar to well characterized GDP-4-keto-6-deoxy-mannose C3/C5 epimerases/C4 reductases involved in GDP-L-fucose synthesis (33, 34). This raises the question of the need for two putative C3/C5 epimerase candidates (Cjj1430 and Cjj1427) to form GDP-6-deoxy-*altro*-heptose when a single C3 epimerization step is required to convert the *manno* sugar configuration of the substrate to the *altro* configuration of the final product. This indicates that the pathway may be more complex than anticipated and/or that the enzymes do not have the anticipated activities. Three different options need to be considered: (i) either Cjj1430 catalyzes both C3 and C5 epimerization steps and Cjj1427 only performs a C5 epimerization, so that the net result of the combined Cjj1430/Cjj1427 catalysis is a C3 epimerization, (ii) or Cjj1430 only catalyzes a C5 epimerization, and Cjj1427 performs both C3 and C5 epimerizations to yield the same net result. (iii) A third option is that Cjj1430 would perform a C3 epimerization and Cjj1427 would not have any epimerization activity. Note that in all three options, Cjj1427 is performing the C4 reduction step as shown by MS.

Cjj1430 Only Has C3 Epimerization Activity—CE analyses indicated that each of Cjj1430 and Cjj1427 makes a single product (Fig. 3, *A* and *C*) but did not provide information as to the identity of the products observed. Likewise, standard MS analyses (Fig. 4) did not allow us to determine the epimerization status of the compounds analyzed, and the exact identity of the Cjj1430 product P4 could not be determined by NMR spectroscopy as this product was too unstable. To decipher whether Cjj1430 performs one or two epimerizations on the heptose substrate, reactions were performed in the presence of deuterated water, and the products obtained were analyzed by MS. In a first set of analyses, the WcbK reaction that supplies substrate to Cjj1430 was performed in deuterated buffer, and Cjj1430 was added once full conversion to P1 had occurred. In control reactions performed with WcbK only, the P1 reaction product obtained in deuterated buffer (referred to as $P1_D$ below) is detected by MS at *m*/*z* 617 (Fig. 6*A*), which is 1 mass unit bigger than P1 formed in H_2O that is detected at *m*/*z* 616 (28). MS/MS showed that this extra mass unit was specifically located on the heptose moiety of the sugar nucleotide as peaks assigned to the GDP moiety were not affected by the presence of deuterium (data not shown). The deuterium incorporation upon reaction with WcbK reflects the well known fact that during the 4,6-dehydratase-catalyzed reaction, there is complete exchange of

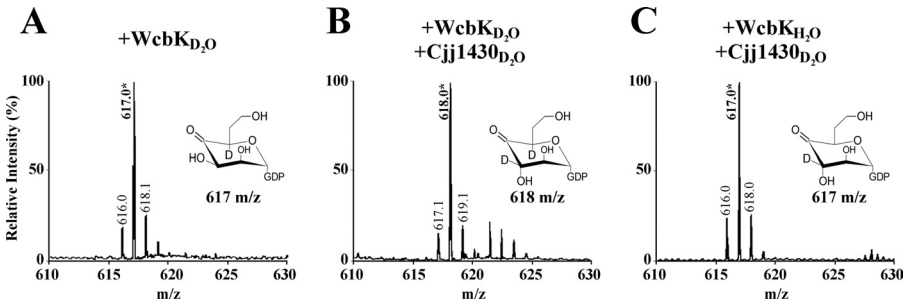

FIGURE 6. **MS/MS spectra of the WcbK and Cjj1430 reaction products obtained in the presence of deuterium to determine the epimerization activity of Cjj1430.** *A,* WcbK product when the reaction was performed in deuterated buffer. *B,* Cjj1430 reaction product when both WcbK and Cjj1430 reactions were performed in deuterium. *C,* Cjj1430 reaction product when the WcbK reaction was done in H_2O, and the Cjj1430 reaction was performed in deuterated buffer.

the C5 proton with solvent hydrogen, which, in deuterated buffer, results in a C5 H/D change (43–45). The characteristics of the $P1_D$ product formed under these conditions can be described as $C5_D$, $C3_H$, and *m*/*z* 617, to account for deuterium incorporation on C5 only.

Upon reaction of this $P1_D$ with Cjj1430 in the presence of deuterated buffer, the reaction product obtained $P4_{DD}$ was detected at *m*/*z* 618 (Fig. 6*B*), which is 2 mass units more than for the Cjj1430 reaction product P4 prepared in H_2O (Fig. 4*A*) and 1 mass unit bigger than the $P1_D$ product. It was confirmed by MS/MS that the second deuterium was also on the heptose ring (data not shown). These data indicate that, in addition to the deuterium atom that was added at C5 by WcbK, Cjj1430 introduced a second deuterium atom in the reaction product. It has been established via conversion of reaction products to alditol acetate prior to MS analysis that C3/C5 epimerases introduce a deuterium atom at both C5 and C3 when reactions are performed in D_2O (30, 46). Therefore, the Cjj1430-mediated introduction of a deuterium to $P1_D$ (where C5 H/D exchange had already taken place via WcbK) indicates C3 epimerization activity of Cjj1430 and results in $P4_{DD}$ ($C5_D$, $C3_D$, *m*/*z* 618).

Because Cjj1430 catalyzes an equilibrium between P1 and P4 in favor of P1, the reaction analyzed by MS contained mostly P1 (~80%). Thus, a significant peak corresponding to $P1_D$ ($C5_D$, $C3_H$, *m*/*z* 617) should *a priori* be expected. However, the Cjj1430-catalyzed back epimerization of P4 into P1 in D_2O results in progressive conversion of the original $P1_D$ product ($C5_D$, $C3_H$, *m*/*z* 617) into $P1_{DD}$ product ($C5_D$, $C3_D$, *m*/*z* 618) via passage through the $P4_{DD}$ intermediate ($C5_D$, $C3_D$, *m*/*z* 618). Therefore, no original $P1_D$ product remained after reaction with Cjj1430 (Fig. 6*B*).

The data above allowed the determination that Cjj1430 has at least C3 epimerization activity. To determine whether it also has C5 epimerization activity, a second set of reactions was performed in which P1 was formed in H_2O (P1 $C5_H$, $C3_H$, *m*/*z* 616), and the Cjj1430 reaction was performed in D_2O. The final reaction also contained ~80% P1, 20% P4, as per CE analysis. By MS, the main product peak was observed at *m*/*z* 617 (Fig. 6*C*). The peak at *m*/*z* 617 includes a product in which a single deuterium has been incorporated. Because we showed in the prior experiment that Cjj1430 has C3 epimerization activity, this peak corresponds to the C3 epimer $P4_D$ ($C5_H$, $C3_D$). If Cjj1430 also had C5 activity, incorporation of two deuterium atoms would have been observed, yielding a peak at *m*/*z* 618. However, no signal was observed at 618 beyond the expected isotopic peak. Therefore, these data indicate that Cjj1430 only has C3 epimerization activity on the heptose substrate.

Further indication that Cjj1430 only has C3 epimerization activity came from the examination of the P1 peak. If Cjj1430 only has C3 epimerase activity, P4 only has a deuterium on C3 ($C5_H$, $C3_D$, *m*/*z* 617). Because of the P1/P4 equilibrium, the back epimerization of P4 into P1 by Cjj1430 would not exchange protons on C5 and would yield only $P1_D$ ($C5_H$, $C3_D$), which is detected at the same *m*/*z* 617 as $P4_D$. This is clearly consistent with what is observed (Fig. 6*C*) as follows: a single main peak at *m*/*z* 617, which includes both $P4_D$ ($C5_H$, $C3_D$) and $P1_D$ ($C5_H$, $C3_D$). If Cjj1430 had both C3 and C5 epimerization activities, two deuteriums would be incorporated, which would generate $P4_{DD}$ ($C5_D$, $C3_D$), which would be detected at *m*/*z* 618. Moreover, the back epimerization of $P4_{DD}$ into P1 would convert all the original P1 ($C5_H$, $C3_H$ at *m*/*z* 616) into $P1_{DD}$ ($C5_D$, $C3_D$), which would also be detected at *m*/*z* 618. Therefore, if Cj1430 performed both C3 and C5 epimerizations, the main peak observed by MS should be at *m*/*z* 618, but this is clearly not what is observed (Fig. 6*C*).

Cjj1427 Only Serves as a Reductase in the GDP-6-Deoxy-altro-heptose Synthesis Pathway—Taken together, the data above conclusively determine that Cjj1430 only has C3 epimerization activity and that its reaction product is therefore GDP-6-deoxy-4-keto-D-*arabino*-heptose, which can lead subsequently to the expected D-*altro*-heptose configuration by simple reduction at C4. Our CE data showed that Cjj1427 converts the Cjj1430 reaction product P4 into P5, which we determined by NMR spectroscopy to be in the *altro* configuration. Because a single C3 epimerization step was required to switch the *manno* configuration of the heptose substrate to the *altro* configuration of the product P5, and Cjj1430 is responsible for this C3 epimerization, the data imply that Cjj1427 does not have any epimerization activity at all but only carries a C4 reduction step to generate the final product P5.

WcaG Is Not Part of the Mainstream GDP-6-Deoxy-D-altro-heptose Synthesis Pathway but Affects Its Outcome—The data presented above raised the question of the role of WcaG in GDP-6-deoxy-*altro*-heptose synthesis, if any. Although Cjj1427-dependent, the activity of WcaG did not use the Cjj1427 product P5 as a substrate but involved the P1 substrate to generate P3, as documented previously (28) and as supported by the data presented in Fig. 3, *A* and *C*. Moreover, the presence of WcaG in reactions containing active WcbK, Cjj1430, and

Cjj1427 led to reduced formation of P5 from GDP-*manno*-heptose (Fig. 3*C*, *traces b* and *d*). This suggests a possible inhibition of Cjj1427 activity by WcaG and/or by the WcaG reaction product P3. The inhibition of Cjj1427 would prevent pulling the Cjj1430 P1/P4 equilibrium toward P4, so there would be more P1 available for catalysis by WcaG. This would result in enhanced formation of P3, as observed. An alternative possibility is that Cjj1427 would enhance WcaG activity, therefore resulting in fast P3 (= P6) formation and reduced P5 formation.

To test the hypothesis of inhibition of Cjj1427 by WcaG and/or P3, a stock of ~75% P1, 25% P4 was generated by reacting GDP-*manno*-heptose with WcbK and Cjj1430 (at equilibrium), and both enzymes were removed by ultrafiltration so that the composition of the P1/P4 stock would remain constant. The P1/P4 stock was then reacted with WcaG only, Cjj1427 only, or with a mix of Cjj1427 and WcaG. Upon reaction with WcaG only, the P1 peak decreased, and the P3 peak appeared as expected (Fig. 7*A*, *trace b*). The P4 peak was not affected. Upon incubation with Cjj1427 only, there was full conversion of P4 into P5 (Fig. 7*A*, *trace c*), but the P1 peak was not affected. The full disappearance of P4, although P1 was still present, also demonstrates that ultrafiltration had been efficient at removing Cjj1430, which would otherwise replenish P4 from P1. Finally, upon incubation with both WcaG and Cjj1427 at once, P4 was still present, P1 decreased, and P3 (= P6) appeared (Fig. 7*A*, *trace d*). The fact that P4 is still present when no replenishment is possible (due to the removal of Cjj1430) clearly demonstrates that Cjj1427 activity had been inhibited by the presence of WcaG and/or its reaction product and that Cjj1427 did not use P4 to generate any intermediate that could serve as a substrate for WcaG. Therefore, these data indicate that, although there is no requirement for WcaG to produce P5, WcaG and/or its product P3 exerts regulatory effects on P5 production via inhibition of Cjj1427 activity.

WcaG Reaction Product P3 Enhances Cjj1427 Activity although WcaG Inhibits Cjj1427—To dissect out which of WcaG or its reaction product P3 inhibited Cjj1427, the effect of addition of purified product P3 on Cjj1427 activity was monitored in reactions comprising GDP-*manno*-heptose, WcbK, Cjj1430, Cjj1427 and cofactor NADPH. Under the conditions tested, no noticeable effect of P3 addition was noted on the activities of WcbK and Cjj1430 (Fig. 7*B, traces b–e*). However, against expectations, the addition of P3 resulted in a significant increase in Cjj1427 activity, as indicated by the increase in peak P5 and total disappearance of the P1 peak (full conversion in *trace g*). The increase in Cjj1427 activity upon P3 addition was also quantified over a wide range of P3 concentrations (up to 0.15 mM) and under conditions where the total substrate was not limiting. P5 formation increased linearly with the amount of P3 added, reaching up to 3-fold under the conditions tested (data not shown). Therefore, altogether these data demonstrate that the addition of P3 in the absence of the WcaG results in enhanced formation of GDP-6-deoxy-D-*altro*-heptose (P5) via enhanced activity of Cjj1427. The effect observed was specific for P3 as no effect of addition of GDP-*manno*-heptose in lieu of P3 was observed (Fig. 7*C*). Note that P3 was not consumed in the process, which is consistent with the fact that P3 is not a substrate for Cjj1427. Overall, these data indicate antagonistic

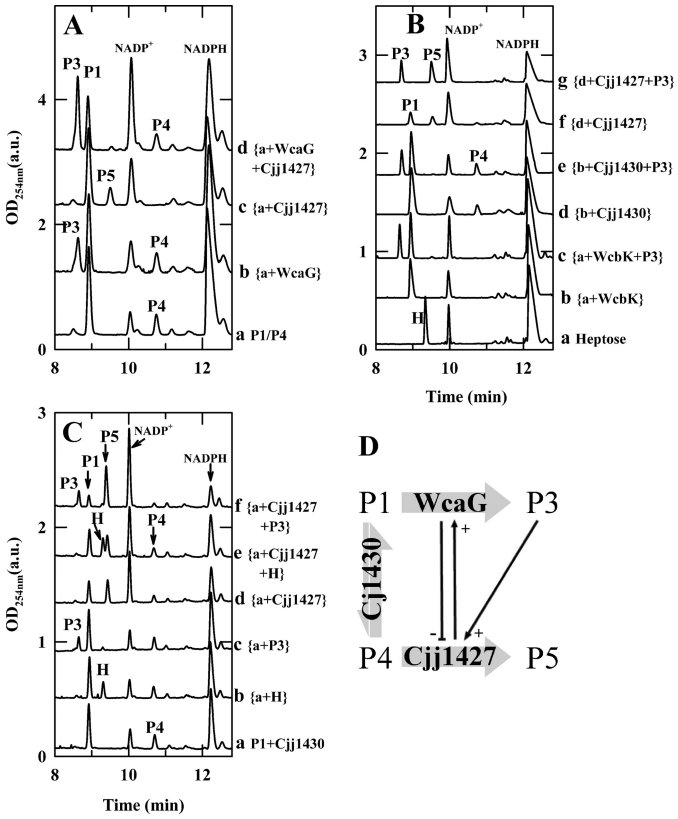

FIGURE 7. **CEs showing the interplay between WcaG, its product P3, and Cjj1427.** *A*, presence of Cjj1427 enhances WcaG activity, and the presence of WcaG inhibits Cjj1427 activity. The reactions were set up with a 0.1 mM of P1/P4 80:20% mixture from which WcbK and Cjj1430 had been removed by ultrafiltration. The reactions were incubated for 16 h with WcaG alone (2.7 pmol, *trace b*), Cjj1427 alone (0.6 pmol, *trace c*), Cjj1427 and WcaG (*trace d*), or none (*trace a*). *B*, P3 affects the activity of Cjj1427 exclusively. Reactions of 5 μl containing 28 pmol of WcbK, 6.3 pmol of Cjj1430, 11.5 pmol of Cjj1427, and 0.16 mM GDP-*manno*-heptose were incubated with or without 0.10 mM purified P3 for 15 min and assessed for formation of the Cjj1427 product P5. Variations in reaction compositions are indicated next to each trace. *C*, activator effect observed on Cjj1427 is specific for P3. Reactions of 5 μl containing 0.1 mM pure P1 and 6.3 pmol of Cjj1430 were incubated with or without 1.15 pmol of Cjj1427 and with or without 0.10 mM purified P3 or GDP-*manno*-heptose (H) for 15 min and assessed for formation of P5. Variations in reaction compositions are indicated next to each trace. *D*, schematic representation of the regulatory loop involving WcaG, Cjj1427, and P3, as highlighted by the CE data presented in *A–C*.

effects of WcaG and its reaction product P3 on Cjj1427 activity. WcaG inhibits Cjj1427 activity, whereas its reaction product P3 enhances Cjj1427 activity (Fig. 7*D*). Whether sufficient amounts of P3 would accumulate *in vivo* for the P3-mediated activation of Cjj1427 to be physiologically relevant is unlikely because full conversion of heptose into P3 (= P6) is readily obtained in the presence of WcaG.

Cjj1427 Activates WcaG—In addition to inhibition of Cjj1427 by WcaG and activation of Cjj1427 by the P3 product, a closer examination of the data presented in Fig. 7*A* indicates that the interplay between WcaG and Cjj1427 also resulted in enhanced activity of WcaG. In reactions performed on the enzyme-free mixture of P1/P4 substrates, limited activity of WcaG was observed in the absence of Cjj1427 under the conditions used for this assay (Fig. 7*A*, *trace b*), but a significant level of WcaG activity was observed in the presence of Cjj1427 (*trace d*). The effect was not due to the Cjj1427 product itself,

because minimal amounts of Cjj1427 product P5 were formed under these assay conditions. Such effects strongly suggest the existence of interactions between WcaG and Cjj1427.

Overall, these data demonstrate the intricacies of the GDP-6-deoxy-*altro*-heptose biosynthetic pathway and its regulatory aspects, with a complex regulatory loop involving Cjj1427, WcaG, and its reaction product P3 (Fig. 7*D*). Against expectations, WcaG activity does not lead to the GDP-6-deoxy-D-*altro*-heptose but prevents its formation and diverts all substrate conversion toward production of GDP-6-deoxy-*manno*-heptose (P3/P6).

DISCUSSION

Challenges in the Elucidation of the GDP-6-Deoxy-D-altro-heptose Biosynthesis Pathway—To the best of our knowledge, this is the first report investigating the complete GDP-6-deoxy-D-*altro*-heptose biosynthetic pathway. The analysis of this pathway was extremely difficult due to the presence of the WcaG side branch with regulatory effects on the activity of Cjj1427 and due to the production of several compounds of identical molecular weight and similar MS/MS spectra. An extra level of complexity came from the fact that Cjj1430 operates in an equilibrium mode, whose direction is opposite to the production of *altro*-heptose. Such unfavorable equilibrium has been observed for hexose C3/C5 epimerases before (30, 47). Finally, several intermediates of the pathway are unstable keto products (P1 and P4) that readily break down to release their GDP moiety, further complicating the analyses. Only very detailed analyses performed with a variety of combinations of enzymes, comparison of data obtained with sequential *versus* concomitant additions of enzymes, processing of all samples extemporaneously (to avoid degradation of unstable intermediates), and analysis of multiple time course series with different enzyme concentrations allowed us to solve this pathway. Also, NMR spectroscopy analyses of the only two stable products of the pathway (P5 and P6) were necessary to allow full elucidation of the pathway and to determine unambiguously that, unexpectedly, P5 was the actual final product of GDP-6-deoxy-D-*altro*-heptose, whereas P6, which was obtained using the four candidate enzymes from the capsule cluster and was anticipated to be the *altro*-heptose derivative, only represented the by-product of the WcaG side branch. Generating enough pure material for these NMR spectroscopy analyses was a major undertaking, considering that generating the GDP-*manno*-heptose substrate from sedoheptulose phosphate requires four enzymatic steps (48), and generating the final P5 and P6 products from the substrate also required multiple enzymatic steps.

Paradox in the GDP-6-Deoxy-D-altro-heptose Biosynthesis Pathway, Two Candidate C3/C5 Epimerases Involved for a Single C3 Epimerization Step—The pathway was anticipated to be fairly straightforward, simply requiring sequential C6 dehydration, C3 epimerization, and C4 reduction of GDP-*manno*-heptose. Our detailed analyses combining CE, MS, and NMR spectroscopy analyses demonstrated that the sequential activities of the C6 dehydratase WcbK (28), putative C3/C5 epimerase Cjj1430, and putative C3/C5 epimerase/C4 reductase Cjj1427 were required to generate GDP-6-deoxy-D-*altro*-heptose from GDP-D-*manno*-heptose. Based on reaction mechanisms of known C3/C5 epimerases, it is expected that Cjj1430 and Cjj1427 perform the necessary epimerization on the heptose while it is still in the 4-keto conformation (30, 33, 34, 49–51), which is consistent with their activity downstream of WcbK.

The requirement for two candidate C3/C5 epimerases (Cjj1430 and Cjj1427) was counter-intuitive because a single C3 epimerization step was necessary. Mass spectrometry analysis of reaction products generated in the presence of deuterium was necessary to resolve the issue. Such experiments have been used previously to characterize the C3/C5 epimerization activities of similar enzymes (30, 50, 51). Our experiments on deuterated reaction compounds clearly demonstrated that Cjj1430 only has C3 epimerization activity on the heptose substrate, which leads to the 4-keto-D-*arabino* sugar intermediate P4 (Fig. 1), and implied that Cjj1427 served as a reductase only. The fact that the P4 reduction step was exclusively carried out by Cjj1427 and that WcaG only reduced P1, which only differs from P1 by its C3 configuration, indicates that the configuration at C3 is a critical determinant of the specificity of these reductases.

It remains a bit of a puzzle that an enzyme such as Cjj1427, with potential for three activities (C3 and C5 epimerase activities and C4 reductase activity) only serves as a reductase, and a potentially bifunctional enzyme such as Cjj1430 only serves as a single epimerase. However, there seems to be an evolutionary component to the current state of the pathway in *C. jejuni* 81-176. In this strain, a C5 epimerization by Cjj1430 would need to be reverted by Cjj1427, therefore resulting in a fairly high energetic cost to switch the configuration back and forth. However, a permanent D to L configuration switch is in fact necessary for the formation of the L-*gluco*-heptose derivative present in *C. jejuni* strain NCTC 11168. This strain harbors a Cj1430 enzyme that is 81% identical and 98% similar to Cjj1430 from strain 81-176. Therefore, both enzymes can be anticipated to perform the same C3 epimerization activity in each strain. In contrast, although strain NCTC 11168 also contains a Cjj1427 homologue (Cj1428), it is only 57% identical and 92% similar to Cjj1427 from strain 81-176. Therefore, Cjj1427 and Cj1428 may differ in their C5 epimerization activities, whereby Cj1428 from NCTC 11168 may perform the necessary C5 epimerization step, although Cjj1427 from strain 81-176 cannot. Obviously, the biochemical activities of these enzymes will be worth investigating to determine whether this is the case.

Complexity in the GDP-6-Deoxy-D-altro-heptose Biosynthesis Pathway, the Cjj1430 P1/P4 Equilibrium, and the WcaG Side Branch—A striking feature of this pathway is the direction of the equilibrium catalyzed by Cjj1430. The equilibrium lies in favor of P1, which is opposite to the direction of the mainstream pathway. Similar observations have been made for other C3/C5 epimerases, such as RmlC (30) and the GDP-mannose 3,5-epimerase (GME) (47). Only the reductase activity of Cjj1427 commits the pathway toward irreversible formation of the final product, effectively pulling the P1/P4 equilibrium toward P4. In the absence of Cjj1427 activity, the pathway would therefore generate copious amounts of P1, which would be readily transformed into P3 by WcaG.

The role of WcaG in this pathway is a puzzle. As schematically represented in Fig. 8, WcaG can reduce an intermediate

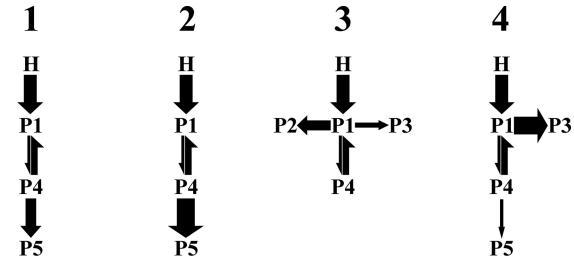

	1	2	3	4
WcbK	+	+	+	+
Cjj1430	+	+	+	+
Cjj1427	+	+	-	+
WcaG	-	-	+	+
Pure P3	-	+	-	-

FIGURE 8. **Schematic representation of the pathway outcomes depending on the experimental setup.** Four different schemes are described (*schemes 1–4*) to highlight the impact of WcaG and its reaction product P3 on GDP-6-deoxy-D-*altro*-heptose synthesis. The addition or omission of enzymes and purified P3 product in the reactions is denoted by + and − signs, respectively. The P3 highlighted in *schemes 3* and *4* was formed during the enzymatic reaction. The *thickness* of the *arrows* reflects the efficiency of the enzymatic step.

(P1) from the GDP-6-deoxy-D-*altro*-heptose synthesis pathway; it affects the activity of Cjj1427 and therefore the outcome of the whole pathway, and it is affected in return by the presence of Cjj1427. Its activity is nevertheless not necessary for GDP-6-deoxy-D-*altro*-heptose synthesis *in vitro*. Because none of the enzymes of the pathway can use P3 as a substrate, P3 cannot merely represent a temporary storage of intermediates for the pathway. In addition, as also schematically represented in Fig. 8, we showed that P3 activates Cjj1427 *in vitro*. Although one could argue that these *in vitro* observations represent mere artifacts, we have observed by knock-out mutagenesis that WcaG is necessary for modified heptose synthesis in *C. jejuni* NCTC 11168.[3] Considering that $WcaG_{NCTC11168}$ is 97% identical to $WcaG_{81\text{-}176}$, it can safely be assumed that $WcaG_{81\text{-}176}$ and the $WcaG_{81\text{-}176}$-dependent side branch that leads to P3 production do have *in vivo* relevance.

Significance of Elucidation of This Pathway—Although C3/C5 epimerases and C3/C5 epimerases/C4 reductases that function on deoxy-hexoses, have attracted much attention for their potential use as antibacterial targets (30, 33, 34, 50, 51), no such enzyme involved in heptose modification pathways has been characterized at the biochemical level to date. These enzymes also represent novel antibacterial targets because they are likely involved in the modification of the heptoses found in virulence-associated surface carbohydrates of a variety of pathogens, including several strains of *C. jejuni* (19, 21, 22), *Campylobacter lari* (52), as well as *Burkholderia* species (53). Also, BLAST searches reveal the presence of non-RmlC and non-GMER homologues (as defined as not identified by BLAST searches performed with the RmlC and GMER protein sequences) of Cjj1430 and Cjj1427 in a variety of bacteria for which the presence of modified heptose has not yet been demonstrated. For example *Helicobacter bilis* and *winghamensis,* several *Serratia* and several *Prevotella* species harbor non-RmlC homologues of Cjj1430 (e values $5e^{-58}$, $1e^{-53}$, $8e^{-24}$, and $1e^{-21}$ respectively), and *Helicobacter hepaticus*, *Francisella philomiragia, Prevotella tannera,* and *Spirochaeta thermophila* harbor non-GMER homologues (e values $1e^{-116}$, $7e^{-114}$, $4e^{-102}$, and $6e^{-112}$, respectively). Therefore, these homologues may also represent novel targets worthy of investigation in pathogenic Helicobacters, Prevotellae, Serratiae, and Francisellae. Inhibitors designed against the *C. jejuni* enzymes characterized in this study may also prove of therapeutic value against these other pathogens.

The data presented in this study will provide a comparison basis that will greatly facilitate the elucidation of similar heptose modification pathways, such as that of the 6-*O*-methyl-L-*gluco*-heptose that is present in *C. jejuni* NCTC 11168. As mentioned above, this pathway is also predicted to involve two candidate C3/C5 epimerases similar to Cjj1430 and Cjj1427 but that are bound to display slight differences in substrate/product specificities. Future structural and site-directed mutagenesis studies will allow defining the molecular basis for substrate specificity in this class of enzymes, which could lead to the rational design of inhibitors.

Overall, beyond the fundamental understanding of the intricacies of this pathway, the information generated in this study has the potential to lead to novel therapeutic or prophylactic agents useful to limit the production of essential virulence factors (capsule or lipopolysaccharide) in a variety of pathogens.

Acknowledgments—We thank Kathy Barber for help preparing some NMR samples and acquisition of NMR data and Dr. Anne Rintala-Dempsey for maintenance of the Biomolecular NMR Facility.

REFERENCES

1. Dasti, J. I., Tareen, A. M., Lugert, R., Zautner, A. E., and Gross, U. (2010) *Campylobacter jejuni*. A brief overview on pathogenicity-associated factors and disease-mediating mechanisms. *Int. J. Med. Microbiol.* **300,** 205–211
2. Kirkpatrick, B. D., and Tribble, D. R. (2011) Update on human *Campylobacter jejuni* infections. *Curr. Opin. Gastroenterol.* **27,** 1–7
3. Poropatich, K. O., Walker, C. L., and Black, R. E. (2010) Quantifying the association between *Campylobacter* infection and Guillain-Barre syndrome. A systematic review. *J. Health Popul. Nutr.* **28,** 545–552
4. Kalischuk, L. D., and Buret, A. G. (2010) A role for *Campylobacter jejuni*-induced enteritis in inflammatory bowel disease? *Am. J. Physiol. Gastrointest. Liver Physiol.* **298,** G1–G9
5. Lindow, J. C., Poly, F., Tribble, D. R., Guerry, P., Carmolli, M. P., Baqar, S., Porter, C. K., Pierce, K. K., Darsley, M. J., Sadigh, K. S., Dill, E. A., Campylobacter Study Team, and Kirkpatrick, B. D. (2010) Caught in the act. *In vivo* development of macrolide resistance to *Campylobacter jejuni* infection. *J. Clin. Microbiol.* **48,** 3012–3015
6. Kittl, S., Kuhnert, P., Hächler, H., and Korczak, B. M. (2011) Comparison of genotypes and antibiotic resistance of *Campylobacter jejuni* isolated from humans and slaughtered chickens in Switzerland. *J. Appl. Microbiol.* **110,** 513–520
7. Zhao, S., Young, S. R., Tong, E., Abbott, J. W., Womack, N., Friedman, S. L., and McDermott, P. F. (2010) Antimicrobial resistance of *Campylobacter* isolates from retail meat in the United States between 2002 and 2007. *Appl. Environ. Microbiol.* **76,** 7949–7956
8. Lin, J., Yan, M., Sahin, O., Pereira, S., Chang, Y. J., and Zhang, Q. (2007) Effect of macrolide usage on emergence of erythromycin-resistant *Campylobacter* isolates in chickens. *Antimicrob. Agents Chemother.* **51,** 1678–1686
9. Monteiro, M. A., Baqar, S., Hall, E. R., Chen, Y. H., Porter, C. K., Bentzel, D. E., Applebee, L., and Guerry, P. (2009) Capsule polysaccharide conjugate vaccine against diarrheal disease caused by *Campylobacter jejuni*.

[3] C. Creuzenet, A. Wong, and D. Lange, unpublished data.

Infect. Immun. **77,** 1128–1136
10. Szymanski, C. M., King, M., Haardt, M., and Armstrong, G. D. (1995) *Campylobacter jejuni* motility and invasion of Caco-2 cells. *Infect. Immun.* **63,** 4295–4300
11. Guerry, P., Ewing, C. P., Schirm, M., Lorenzo, M., Kelly, J., Pattarini, D., Majam, G., Thibault, P., and Logan, S. (2006) Changes in flagellin glycosylation affect *Campylobacter* autoagglutination and virulence. *Mol. Microbiol.* **60,** 299–311
12. Szymanski, C. M., Yao, R., Ewing, C. P., Trust, T. J., and Guerry, P. (1999) Evidence for a system of general protein glycosylation in *Campylobacter jejuni*. *Mol. Microbiol.* **32,** 1022–1030
13. Szymanski, C. M., Burr, D. H., and Guerry, P. (2002) *Campylobacter* protein glycosylation affects host cell interactions. *Infect. Immun.* **70,** 2242–2244
14. Guerry, P., Szymanski, C. M., Prendergast, M. M., Hickey, T. E., Ewing, C. P., Pattarini, D. L., and Moran, A. P. (2002) Phase variation of *Campylobacter jejuni* 81-176 lipooligosaccharide affects ganglioside mimicry and invasiveness *in vitro*. *Infect. Immun.* **70,** 787–793
15. Bacon, D. J., Szymanski, C. M., Burr, D. H., Silver, R. P., Alm, R. A., and Guerry, P. (2001) A phase-variable capsule is involved in virulence of *Campylobacter jejuni* 81-176. *Mol. Microbiol* **40,** 769–777
16. Keo, T., Collins, J., Kunwar, P., Blaser, M. J., and Iovine, N. M. (2011) *Campylobacter* capsule and lipooligosaccharide confer resistance to serum and cationic antimicrobials. *Virulence* **2,** 30–40
17. Guerry, P., and Szymanski, C. M. (2008) *Campylobacter* sugars sticking out. *Trends Microbiol.* **16,** 428–435
18. Karlyshev, A. V., Champion, O. L., Churcher, C., Brisson, J. R., Jarrell, H. C., Gilbert, M., Brochu, D., St Michael, F., Li, J., Wakarchuk, W. W., Goodhead, I., Sanders, M., Stevens, K., White, B., Parkhill, J., Wren, B. W., and Szymanski, C. M. (2005) Analysis of *Campylobacter jejuni* capsular loci reveals multiple mechanisms for the generation of structural diversity and the ability to form complex heptoses. *Mol. Microbiol.* **55,** 90–103
19. Aspinall, G. O., McDonald, A. G., and Pang, H. (1992) Structures of the O chains from lipopolysaccharides of *Campylobacter jejuni* serotypes O:23 and O:36. *Carbohydr. Res.* **231,** 13–30
20. Aspinall, G. O., Lynch, C. M., Pang, H., Shaver, R. T., and Moran, A. P. (1995) Chemical structures of the core region of *Campylobacter jejuni* O:3 lipopolysaccharide and an associated polysaccharide. *Eur. J. Biochem.* **231,** 570–578
21. Chen, Y. H., Poly, F., Pakulski, Z., Guerry, P., and Monteiro, M. A. (2008) The chemical structure and genetic locus of *Campylobacter jejuni* CG8486 (serotype HS:4) capsular polysaccharide. The identification of 6-deoxy-D-*ido*-heptopyranose. *Carbohydr. Res.* **343,** 1034–1040
22. St Michael, F., Szymanski, C. M., Li, J., Chan, K. H., Khieu, N. H., Larocque, S., Wakarchuk, W. W., Brisson, J. R., and Monteiro, M. A. (2002) The structures of the lipooligosaccharide and capsule polysaccharide of *Campylobacter jejuni* genome sequenced strain NCTC 11168. *Eur. J. Biochem.* **269,** 5119–5136
23. Kanipes, M. I., Papp-Szabo, E., Guerry, P., and Monteiro, M. A. (2006) Mutation of waaC, encoding heptosyltransferase I in *Campylobacter jejuni* 81-176, affects the structure of both lipooligosaccharide and capsular carbohydrate. *J. Bacteriol.* **188,** 3273–3279
24. Bachtiar, B. M., Coloe, P. J., and Fry, B. N. (2007) Knockout mutagenesis of the *kpsE* gene of *Campylobacter jejuni* 81116 and its involvement in bacterium-host interactions. *FEMS Immunol. Med. Microbiol.* **49,** 149–154
25. Ho, N., Kondakova, A. N., Knirel, Y. A., and Creuzenet, C. (2008) The biosynthesis and biological role of 6-deoxyheptose in the lipopolysaccharide O-antigen of *Yersinia pseudotuberculosis*. *Mol. Microbiol.* **68,** 424–447
26. Kondakova, A. N., Ho, N., Bystrova, O. V., Shashkov, A. S., Lindner, B., Creuzenet, C., and Knirel, Y. A. (2008) Structural studies of the O-antigens of *Yersinia pseudotuberculosis* O:2a and mutants thereof with impaired 6-deoxy-D-manno-heptose biosynthesis pathway. *Carbohydr. Res.* **343,** 1383–1389
27. Peng, W., Jayasuriya, A. B., Imamura, A., and Lowary, T. L. (2011) Synthesis of the 6-*O*-methyl-D-glycero-α-L-*gluco*-heptopyranose moiety present in the capsular polysaccharide from *Campylobacter jejuni* NCTC 11168. *Org. Lett.* **13,** 5290–5293
28. McCallum, M., Shaw, G. S., and Creuzenet, C. (2011) Characterization of the dehydratase WcbK and the reductase WcaG involved in GDP-6-deoxy-*manno*-heptose biosynthesis in *Campylobacter jejuni*. *Biochem. J.* **439,** 235–248
29. Butty, F. D., Aucoin, M., Morrison, L., Ho, N., Shaw, G., and Creuzenet, C. (2009) Elucidating the formation of 6-deoxyheptose. Biochemical characterization of the GDP-D-glycero-D-*manno*-heptose C6 dehydratase, DmhA, and its associated C4 reductase, DmhB. *Biochemistry* **48,** 7764–7775
30. Stern, R. J., Lee, T. Y., Lee, T. J., Yan, W., Scherman, M. S., Vissa, V. D., Kim, S. K., Wanner, B. L., and McNeil, M. R. (1999) Conversion of dTDP-4-keto-6-deoxyglucose to free dTDP-4-keto-rhamnose by the *rmlC* gene products of *Escherichia coli* and *Mycobacterium tuberculosis*. *Microbiology* **145,** 663–671
31. Xiang, S. H., Haase, A. M., and Reeves, P. R. (1993) Variation of the *rfb* gene clusters in. *Salmonella enterica*. *J. Bacteriol.* **175,** 4877–4884
32. Yao, Z., and Valvano, M. A. (1994) Genetic analysis of the *O*-specific lipopolysaccharide biosynthesis region (rfb) of *Escherichia coli* K-12 W3110. Identification of genes that confer group 6 specificity to *Shigella flexneri* serotypes Y and 4a. *J. Bacteriol.* **176,** 4133–4143
33. Rizzi, M., Tonetti, M., Vigevani, P., Sturla, L., Bisso, A., Flora, A. D., Bordo, D., and Bolognesi, M. (1998) GDP-4-keto-6-deoxy-D-mannose epimerase/reductase from *Escherichia coli*, a key enzyme in the biosynthesis of GDP-L-fucose, displays the structural characteristics of the RED protein homology superfamily. *Structure* **6,** 1453–1465
34. Järvinen, N., Mäki, M., Räbinä, J., Roos, C., Mattila, P., and Renkonen, R. (2001) Cloning and expression of *Helicobacter pylori* GDP-L-fucose synthesizing enzymes (GMD and GMER) in *Saccharomyces cerevisiae*. *Eur. J. Biochem.* **268,** 6458–6464
35. Newton, D. T., and Mangroo, D. (1999) Mapping the active site of the *Haemophilus influenzae* methionyl-tRNA formyltransferase. Residues important for catalysis and tRNA binding. *Biochem. J.* **339,** 63–69
36. Smallcombe, S. H., Patt, S. L., and Keifer, P. A. (1995) WET solvent suppression and its applications to LC NMR and high resolution NMR spectroscopy. *J. Magn. Reson.* **A117,** 295–303
37. Bax, A., and Davis, D. G. (1985) MLEV-17-based two-dimensional homonuclear magnetization transfer spectroscopy. *J. Magn. Reson.* **65,** 355–360
38. Kay, L. E., Keifer, P., and Saarinen, T. (1992) Pure absorption gradient enhanced heteronuclear single quantum correlation spectroscopy with improved sensitivity. *J. Am. Chem. Soc.* **114,** 10663–10665
39. John, B. K., Plant, D., and Hurd, R. E. (1992) Improved proton-detected heteronuclear correlation using gradient-enhanced z and zz filters. *J. Magn. Reson.* **A101,** 113–117
40. Creuzenet, C., Belanger, M., Wakarchuk, W. W., and Lam, J. S. (2000) Expression, purification, and biochemical characterization of WbpP, a new UDP-GlcNAc C_4 epimerase from *Pseudomonas aeruginosa* serotype O6. *J. Biol. Chem.* **275,** 19060–19067
41. Creuzenet, C., Schur, M. J., Li, J., Wakarchuk, W. W., and Lam, J. S. (2000) FlaA1, a new bifunctional UDP-GlcNAc C_6 dehydratase/C_4 reductase from *Helicobacter pylori*. *J. Biol. Chem.* **275,** 34873–34880
42. Shashkov, A. S., Pakulski, Z., Grzeszczyk, B., and Zamojski, A. (2001) Distribution of pyranose and furanose forms of 6-deoxyheptoses in water solution. *Carbohydr. Res.* **330,** 289–294
43. Gabriel, O., and Lindquist, L. C. (1968) Biological mechanisms involved in the formation of deoxy sugars. IV. Enzymatic conversion of thymidine diphosphoglucose-4T to thymidine diphospho-4-keto-6-deoxyglucose-6T. *J. Biol. Chem.* **243,** 1479–1484
44. Melo, A., Elliott, W. H., and Glaser, L. (1968) The mechanism of 6-deoxyhexose synthesis. I. Intramolecular hydrogen transfer catalyzed by deoxythymidine diphosphate D-glucose oxidoreductase. *J. Biol. Chem.* **243,** 1467–1474
45. Hegeman, A. D., Gross, J. W., and Frey, P. A. (2002) Concerted and stepwise dehydration mechanisms observed in wild-type and mutated *Escherichia coli* dTDP-glucose 4,6-dehydratase. *Biochemistry* **41,** 2797–2804
46. Melo, A., and Glaser, L. (1968) The mechanism of 6-deoxyhexose synthesis. II. Conversion of deoxythymidine diphosphate 4-keto-6-deoxy-D-glucose to deoxythymidine diphosphate L-rhamnose. *J. Biol. Chem.* **243,** 1475–1478

47. Major, L. L., Wolucka, B. A., and Naismith, J. H. (2005) Structure and function of GDP-mannose-3′,5′-epimerase. An enzyme which performs three chemical reactions at the same active site. *J. Am. Chem. Soc.* **127,** 18309–18320
48. Kneidinger, B., Graninger, M., Puchberger, M., Kosma, P., and Messner, P. (2001) Biosynthesis of nucleotide-activated D-*glycero*-D-*manno*-heptose. *J. Biol. Chem.* **276,** 20935–20944
49. Ito, S. (2009) Features and applications of microbial sugar epimerases. *Appl. Microbiol. Biotechnol.* **84,** 1053–1060
50. Dong, C., Major, L. L., Srikannathasan, V., Errey, J. C., Giraud, M. F., Lam, J. S., Graninger, M., Messner, P., McNeil, M. R., Field, R. A., Whitfield, C., and Naismith, J. H. (2007) RmlC, a C3′ and C5′ carbohydrate epimerase, appears to operate via an intermediate with an unusual twist boat conformation. *J. Mol. Biol.* **365,** 146–159
51. Lau, S. T., and Tanner, M. E. (2008) Mechanism and active site residues of GDP-fucose synthase. *J. Am. Chem. Soc.* **130,** 17593–17602
52. Aspinall, G. O., Monteiro, M. A., Pang, H., Kurjanczyk, L. A., and Penner, J. L. (1995) Lipo-oligosaccharide of *Campylobacter lari* strain PC 637. Structure of the liberated oligosaccharide and an associated extracellular polysaccharide. *Carbohydr. Res.* **279,** 227–244
53. Reckseidler, S. L., DeShazer, D., Sokol, P. A., and Woods, D. E. (2001) Detection of bacterial virulence genes by subtractive hybridization. Identification of capsular polysaccharide of *Burkholderia pseudomallei* as a major virulence determinant. *Infect. Immun.* **69,** 34–44